Journal of CO2 Utilization 82 (2024) 102754

Contents lists available at ScienceDirect

Journal of CO2 Utilization

journal homepage: www.elsevier.com/locate/jcou

Enzymatic conversion of CO_2 to formate: The potential of tungsten-containing formate dehydrogenase in flow reactor system

Byoung Wook Jeon [a,1], Uyen Thu Phan [a,1], Yoonyoung Heo [b], Hyung Ho Lee [b], Jungki Ryu [a,c,*], Yong Hwan Kim [a,**]

[a] School of Energy and Chemical Engineering and Graduate School of Carbon Neutrality, Ulsan National Institute of Science and Technology, 50, UNIST-gil, Eonyang-eup, Ulju-gun, Ulsan, Republic of Korea

[b] Department of Chemistry, Department of Energy Engineering, College of Natural Sciences, Seoul National University, 1, Gwanak-ro, Gwanak-gu, Seoul, Republic of Korea

[c] Ulsan National Institute of Science and Technology, 50, UNIST-gil, Eonyang-eup, Ulju-gun, Ulsan, Republic of Korea

ARTICLE INFO

Keywords:
Methylorubrum extorquens AM1
Formate dehydrogenase 1 (MeFDH1)
Enzymatic CO_2 conversion
Flow reactor
in-situ separation

ABSTRACT

This study introduces a novel approach for CO_2 reduction to formate using the recombinant formate dehydrogenase 1 (MeFDH1) from *Methylorubrum extorquens* AM1 as biocatalyst, addressing challenges in activity, productivity, and long-term stability of enzyme. We demonstrate that immobilized MeFDH1 supported by electrochemical reaction system enhances formate production and stability, achieving over 1.7 M concentration with an initial rate of 20 mM/h and near-unity Faradaic efficiency for over 200 hours. In further, the reusability of immobilized MeFDH1 was obtained without significant declination of productivity and selectivity. The electrochemical study of MeFDH1 found the product inhibition in continuous CO_2 conversion. To overcome this challenge and build efficient process, the integration of a flow reactor system and *in-situ* separation unit further improved the system's performance and scalability. This advancement in enzymatic CO_2 conversion suggests the potential of biocatalysis towards addressing global warming through sustainable chemical synthesis.

1. Introduction

Conversion of carbon dioxide (CO_2) serves as a vital technology for its fixation and utilization of greenhouse gases in the production of various chemicals [1]. Formate has garnered interest due to its higher energy efficiency and technically straightforward production from CO_2 [2]. Presently, the annual production of formate exceeds 720,000 tons, with well-established applications in the chemical and agricultural industries [3]. Moreover, formate and formic acid are rising for bioavailability as sole carbon source [4,5] to produce value-added biomaterial such as bioplastic [6], microbial proteins [7,8], and pharmaceuticals [9] as well as for promising hydrogen carriers owing to their condensed nature [10,11]. The electrochemical production of formate from CO_2 is typically conducted using expensive noble (Pd, Bi) or post-transition (Pb) metal catalysts [12–14]. However, these catalysts are limited by high applied potential, low selectivity, and susceptibility to impurities from CO_2 sources (e.g., SOx, NOx, and O_2), while the excellent performance of the reaction system enables CO_2 reduction with high productivity reaching Ampere-scale [15–18]. These state-of-the-art electrochemical systems for CO_2 reduction for formate have been validated for industrial applicability, and consumed electrolyzer electricity and separation strategies are emerging as key determinants of operating costs. [19,20]. Notably, Bi- or In-based catalysts achieved the highest current density with approximately 1 A/cm^2 and $>$ 90% of Faradaic efficiency (FE) as the industrial-scale performance, albeit requiring over -1.6 V and -2.5 V vs reversible hydrogen electrode (RHE), respectively [21,22]. Fan et al. developed an *in-situ* separation architecture of an all-solid-state reactor to produce highly pure formic acid through humidified nitrogen gas flow. While this Bi-catalyzed reaction system successfully obtained over 15 M of pure formic acid, highly concentrated formic acid nearby the cathode led to significant declination of Faradaic efficiency up to 40% [23]. These findings implied that an efficient

* Corresponding author at: School of Energy and Chemical Engineering and Graduate School of Carbon Neutrality, Ulsan National Institute of Science and Technology, 50, UNIST-gil, Eonyang-eup, Ulju-gun, Ulsan, Republic of Korea.

** Corresponding author.

E-mail addresses: jryu@unist.ac.kr (J. Ryu), metalkim@unist.ac.kr (Y.H. Kim).

[1] These authors contributed equally to this work.

https://doi.org/10.1016/j.jcou.2024.102754

Received 4 January 2024; Received in revised form 23 March 2024; Accepted 25 March 2024

separation strategy not only impacts operating costs to be lower but also maintains its selectivity, ensuring the high value of FE. In contrast, biocatalysts such as microbial metal containing formate dehydrogenase (FDH) exhibit higher turnover frequency, superior selectivity with near-unity Faradaic efficiency, and lower overpotential while requiring milder operating conditions. Consisting of proteins and inexpensive, abundant metal elements (e.g., Mo and W) found within microorganisms, FDH emerges as a promising biocatalyst for electrochemical CO_2 reduction and inspired to develop other type of metal catalysts [24,25]. Despite these advantages, the progress of FDH-catalyzed formate production has been slow and confined to the laboratory scale due to inherent drawbacks of most biocatalysts, such as rapid reverse reactions (formate oxidation) [26–28]. To date, only sub-millimolar scale formate or conceptual studies have been achieved using FDHs [29].

Previous studies on whole-cell biocatalysis and genetic engineering of *Methylorubrum extorquens* AM1 have demonstrated the pivotal role played by MeFDH1 in reducing CO_2 into formate [30–32]. To produce this recombinant enzyme efficiently, microbial engineering of this strain was implemented. Firstly, a knock-out strain (*Δfdh1ba*) of *M. extorquens* AM1 was prepared to avoid complementary interaction between identical MeFDH1-encoding gene on the genome and recombinant expression system for the stability of the plasmid [33]. And, then its homologous recombinant expression plasmid with a methanol-inducible promoter (P_{mxaF}) was applied [34].

In this study, we report a highly efficient enzymatic CO_2 conversion to formate using a tungsten-containing MeFDH1 (formate dehydrogenase 1 from *Methylorubrum extorquens* AM1), addressing the limitations of prior approaches. Considering the kinetic analysis of MeFDH1 with respect to CO_2 and electron mediator, it was demonstrated that high kinetic efficiency of recombinant MeFDH1 is promising for enzymatic CO_2 conversion. Electrochemical reactor supplied the reduced ethyl viologen ($EV^{\bullet+}$) as electron mediator to convert CO_2 into formate continuously for high concentration. For the enhanced applicability of MeFDH1, continuous flow reactor system was built to enable efficient modulation of each component in the process. The integration of *in-situ* separation unit allowed this flow reactor to be maintained initial productivity for long-term operation.

2. Materials and methods

2.1. Instruments, biochemicals, and chemicals

Unless stated otherwise, all chemical reagents for culture, protein purification, and enzymatic assays were purchased from Sigma-Aldrich and used without further purification. Wild-type *Methylorubrum extorquens* AM1 (ATCC 14718, GenBank accession No. CP001510.1) was used to develop a homologous recombinant expression host for the preparation of formate dehydrogenase 1 (MeFDH1, GenBank for alpha and beta: ACS42636.1 and ACS42635.1). pCM184 (GenBank: AY093429.1) and pCM157(Addgene, 45863), used for gene knockout in the genome of the strain, and pCM110 (GenBank: AF327718.1), used for methanol-inducible expression regulated by the promoter P_{mxaF}, were obtained from Addgene (Watertown, MA, USA). The T4 DNA polymerase, restriction enzymes, and their buffers were acquired from New England Biolabs (NEB) and TaKaRa. For culture, the minimal salt medium contained major nutrients (1.62 g/L NH_4Cl, 0.2 g/L $MgSO_4$, 2.21 g/L K_2HPO_4, and 1.25 g/L $NaH_2PO_4{\bullet}2\ H_2O$), trace elements (15 mg/L $Na_2EDTA_2{\bullet}H_2O$, 4.5 mg/L $ZnSO_4{\bullet}7\ H_2O$, 0.3 mg/L $CoCl_2{\bullet}6\ H_2O$, 1 mg/L $MnCl_2{\bullet}4\ H_2O$, 1 mg/L H_3BO_3, 2.5 mg/L $CaCl_2$, 0.4 mg/L $Na_2MoO_4{\bullet}2\ H_2O$, 3 mg/L $FeSO_4{\bullet}7\ H_2O$, and 0.3 mg/L $CuSO_4{\bullet}5\ H_2O$), 30 μM disodium tungstate, 16 g/L disodium succinate hexahydrate as the sole carbon source, and 0.5% methanol for induction of the recombinant expression system [35]. The following antibiotics were applied at the stated concentrations to select transformants: rifamycin (50 mg/L), kanamycin (20 mg/L), and tetracycline (20 mg/L). Affinity chromatography was carried out on a Ni-NTA resin (QIAGEN, Hilden, Germany) for protein purification. To quantify the concentration of the purified MeFDH1, the absorbance at 280 nm was measured on a Nanodrop instrument (Thermo Scientific, Waltham, MA, USA), and an extinction coefficient of 8.89 $L{\bullet}mg^{-1}cm^{-1}$ for a 1% (i.e., 10 mg/mL) dilution was calculated by EMBOSS pepstats. All experimental data for kinetic, stability, and pH dependence analyses were obtained by means of UV/vis spectrometers (Cary 60 by Agilent, Santa Clara, CA, USA) in an anaerobic chamber and UV-1650PC by Shimadzu (Kyoto, Japan) in aerobic conditions equipped with a temperature controller.

2.2. Kinetic study of MeFDH1

Kinetic analysis was conducted to determine kinetic properties of MeFDH1 for CO_2 reduction. EV, an artificial electron mediator, was used to measure the rates of CO_2 reduction catalyzed by MeFDH1 or RcFDH. Reduced EV ($EV^{\bullet+}$) was detected at 600 nm through UV/Vis spectroscopy and had an extinction coefficient of 10.220 $mM^{-1}cm^{-1}$. Because $EV^{\bullet+}$ can be oxidized by oxygen molecules, all kinetic analyses using EV were implemented in an anaerobic chamber. The assay solution was composed of 200 mM-potassium phosphate, 3–100 mM potassium bicarbonate, and 0.015–0.12 mM $EV^{\bullet+}$. Potassium bicarbonate was used as the CO_2 source and converted to dissolved CO_2 due to the pH of enzyme assay at pH 6.3. The concentrations of aqueous CO_2, bicarbonate, and carbonate were calculated by Eq. 1a, Eq. 1b, and Eq. 1c with the total concentration of CO_2 species (c) and the dissociation constants of $pK_{a1} = 6.3$ and $pK_{a2} = 10.3$ [36].

$$[CO_2(aq)] = \frac{c \bullet [H^+]^2}{[H^+]^2 + [H^+]{\bullet}K_{a1} + K_{a1} \bullet K_{a2}} \tag{1a}$$

$$\left[HCO_3^-\right] = \frac{c \bullet [H^+]{\bullet}K_{a1}}{[H^+]^2 + [H^+] \bullet K_{a1} + K_{a1} \bullet K_{a2}} \tag{1b}$$

$$\left[CO_3^{2-}\right] = \frac{c \bullet K_{a1}{\bullet}K_{a2}}{[H^+]^2 + [H^+]{\bullet}K_{a1} + K_{a1} \bullet K_{a2}} \tag{1c}$$

Therefore, the concentration of aqueous CO_2 was determined from the added bicarbonate concentration and the pH. A bicarbonate stock solution was prepared immediately before use due to its dissociation into CO_2. EV was reduced by adding zinc metal at a 5-fold molar excess over EV [23]. Then, the remaining zinc metal was immediately eliminated using a 0.2 μm syringe filter because excessive exposure would allow EV to dimerize in an inactive form.

The kinetic parameters of MeFDH1 for CO_2 reduction with EV were analyzed by Lineweaver-Burk plots and a two-substrate *bi-bi* mechanism model (Fig. S3) [37]. To determine the ratio of active FDH in this study, all turnover rates of MeFDH1 and RcFDH were normalized with the number of active site (W/Mo-bis-MGD), respectively.

2.3. Electrochemical reactor for continuous CO_2 reduction of MeFDH1

The electrochemical CO_2 reduction procedure was described in a previous paper [31]. The electrochemical reactor includes a three-electrode system consisting of carbon felt (2.0 cm × 1.5 cm, AvCarb G300A) and a reference electrode (Ag/AgCl, MF-2079, BASi) in the cathode section and a Pt wire for water splitting in the anode section. A 100 mM H_2SO_4 solution was used to generate electrons and protons on the Pt wire electrode. A Nafion® 115 membrane (0.005 in.) separated the anode section and cathode section and allowed only protons to pass through. The cathodic electrolyte was composed of 200 mM potassium phosphate (pH 7) and 10 mM EV purged by high-purity CO_2 gas (99.999%) with a 30 mL working volume. Unless stated otherwise, purging gases were supplied to the electrochemical cell after oxygen removal with an Agilent BOT-2 O_2 trap. Cyclic voltammograms were measured with 0.1 mM of EV and 60 U MeFDH1 under the following condition: potential range from −0.5 V to −0.8 V vs Ag/AgCl and a scan

rate of 20 mV/s. To investigate potential-dependent catalytic activity of MeFDH1, chronoamperometry was conducted at various potentials with 10 mM of EV and 60 U of MeFDH1 after CO_2 purging for 30 min. The formate concentration and Faradaic efficiency was measured after electrochemical CO_2 reduction for 10 min. The electrode potential (-0.50 V to −0.84 V vs. Ag/AgCl) was consistently controlled by a potentiometer (MultiEnStat3, PalmSens). For long-term operational stability in electrochemical CO_2 reduction, MeFDH1 was immobilized on Ni-NTA agarose, and Ni-NTA agarose beads were added to the lysate. Ni-NTA agarose was loaded into an empty gravity flow column (Bio-Rad, Cat No. 7321010) and washed with binding buffer. The specific activity of MeFDH1 immobilized on Ni-NTA agarose was determined after the elution of MeFDH1 by elution buffer (50 mM MOPS/KOH and 300 mM imidazole at pH 7.0). A total of 250 U of immobilized MeFDH1 was equilibrated with 3-folds resin volume of cathodic electrolyte (200 mM-potassium phosphate buffer at pH 7.0) by flow-through washing and then used for electrochemical reduction of CO_2 to formate. To verify the reusability of immobilized MeFDH1, beads were loaded into an empty column in an anaerobic chamber to wash away the electron mediator and formate to minimize undesired reactions of $EV^{\bullet+}$, such as the generation of reactive oxygen species. Intermittent addition of formate during CO_2 conversion was implemented for demonstrating product inhibition. 6 M of potassium formate (pH 6.3) was prepared and purged CO_2 before use. This solution was added at each 40 min intervals to increase the formate concentration in the cathode section for current measurements. 200 μL of electrolyte was collected to measure actual formate concentration before and after formate addition. To measure the concentration of formate produced by CO_2 reduction, samples were quenched by 540 mM H_2SO_4 and analyzed using HPLC. This analysis was carried out using an Aminex HPX 87-H column and a refractive index detector (RID) with a mobile phase of 5 mM H_2SO_4 (flow rate: 0.6 mL/min).

2.4. Architecture of flow reactor system of enzymatic CO_2 conversion

Overall process of flow reactor system was represented in Fig. 4a, S4a and S6. All units (e.g., MeFDH1-packed bed column, AIEX column, electrolyser) was connected by Poly Ether Ketone (PEEK) tubing (IDEX Health & Science LLC) with outer diameter of 1/16 and 1/8 inch. Peristaltic pump (BT100–1 L, Longer) allowed circular flow (5 mL/min) between MeFDH1-packed bed column and electrolyser to transfer reduced $EV^{\bullet+}$ and dissolved CO_2 for continuous formate production. Due to wear, Tygon® tubing (E3603, Masterflex) was periodically replaced. 50 mL of electrolyte (200 mM-potassium phosphate at pH 7.0) was added into cathode section and 10 mM of EV was considered

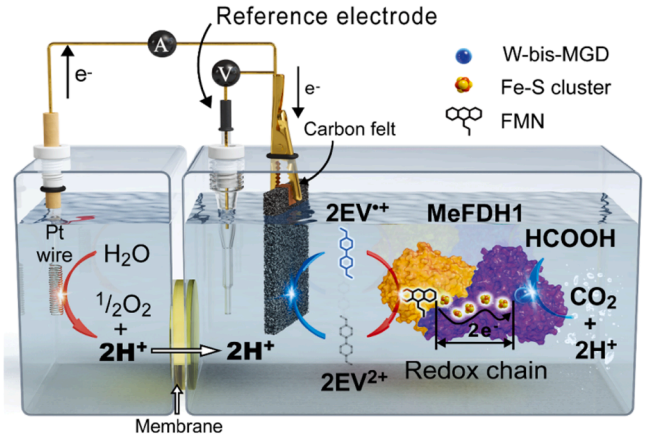

Fig. 1. Scheme of MeFDH1-catalyzed electrochemical CO_2 reduction reaction. MeFDH1 (PDB ID: 7VW6) is composed of alpha (purple) and beta (yellow) subunits with cofactors.

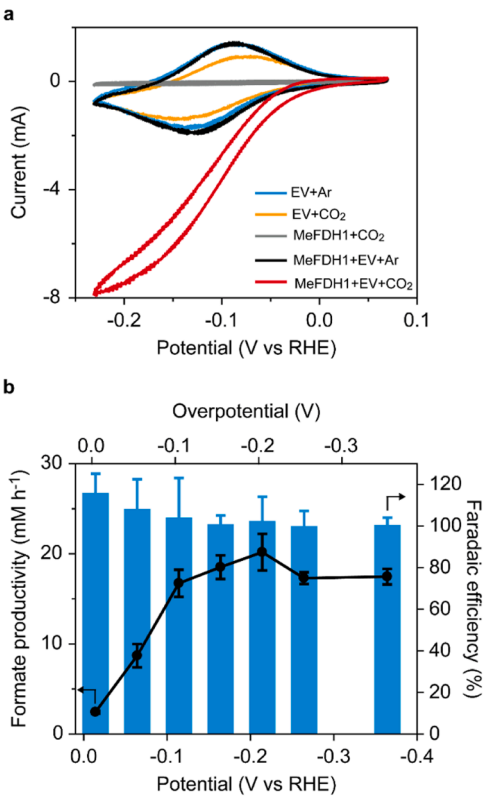

Fig. 2. MeFDH1-catalyzed electrochemical CO_2 reduction. (a) Cyclic voltammograms demonstrate that CO_2 is converted into formate by MeFDH1 using reduced $EV^{\bullet+}$. (b) Electrochemical properties of free MeFDH1 for CO_2 reduction to formate.

containing total volume of flow reactor system. 4 mL of MeFDH1 (250 U) immobilized on Ni-NTA agarose beads was packed into commercial plug flow column (HiScale 16/20, Cytiva). 45 g of Anion exchange resin (Ambersep 900® hydroxide form, Sigma-Aldrich) was also loaded on commercial column (XK 26/40, Cytiva) and distillated water was flowed to wash the resin. The assembly of electrolyser was coincident with that of batch system, and additional tubing for flowing electrolyte was only installed. Flow-through cuvette with path length of 0.01 mm and 0.1 mm (Hellma) was equipped in each side of MeFDH1-packed column, respectively and UV/Vis spectroscopy (UV5, Mettler Toledo) measured the concentration of reduced $EV^{\bullet+}$ in the cuvette. After all units was equipped in flow reactor system, CO_2-saturated buffer was flowed to equilibrate the reaction system for 1 hour prior to reaction initiation. The reaction was initiated with applied bias as −0.164 V vs RHE. The elution of produced formate from AIEX column was conducted after detachment from flow reactor system and distilled water of 350 mL (5 CV) with 3 mL/min was passed through the AIEX column at a flow rate of 3 mL/min, serving as an unbound washing step. Following the washing step, formate was then eluted using 1 N-NaOH of 380 mL (5.4 CV) at the same flow rate. Each 5 mL of fraction was collected during this elution process and analyzed to determine the concentration of formate.

3. Results and discussion

3.1. Enzymatic kinetic and electrochemical analysis of MeFDH1 for CO_2 conversion

Recombinant MeFDH1 was composed of α and β subunits, with the α subunit incorporating a C-terminal His tag (His6) for one-step purification and/or immobilization, unlike other multi-step purification processes (Fig. S1 and Table S1) [39,40]. This enzyme contains

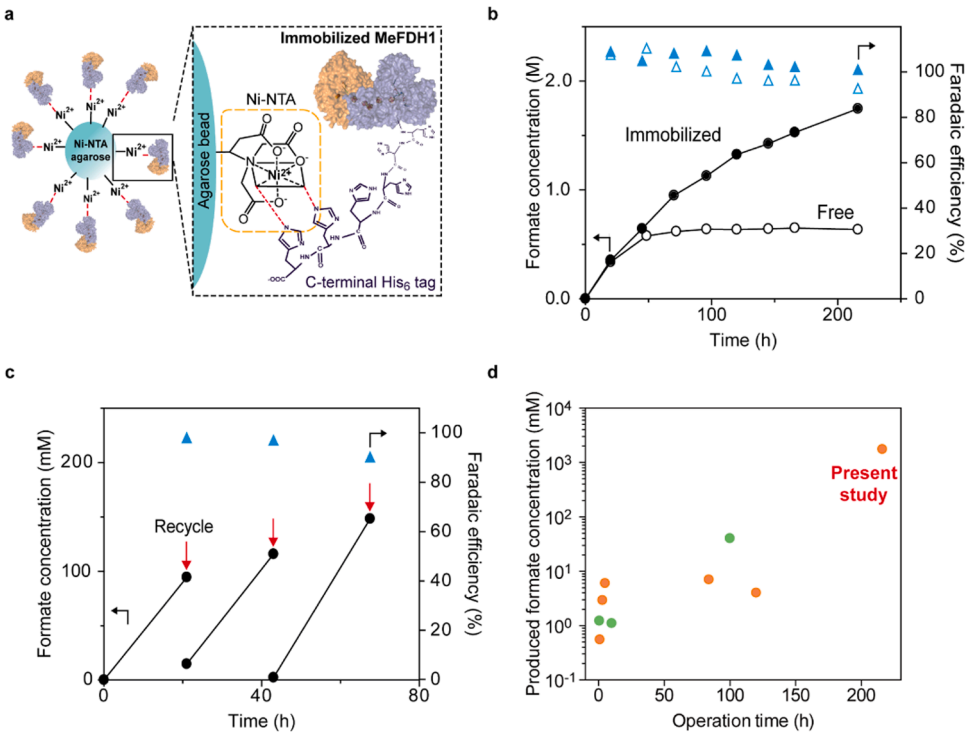

Fig. 3. Long-term stability of MeFDH1-catalyzed CO_2 conversion in batch system. (a) Scheme of immobilization of recombinant MeFDH1-His6 on Ni-NTA agarose. (b) Long-term operation of electrochemical CO_2 reduction by MeFDH1: free vs. immobilized MeFDH1 (open vs. closed symbols). (c) Reusability of immobilized MeFDH1. All the electrochemical reactions were performed at −0.164 V at pH 6.3. (d) Recent progress of enzymatic CO_2 conversion compared with MeFDH1-catalyzed CO_2 reduction. Reaction type: electrochemistry (orange) and cascade enzyme reaction (green). The in-detailed characteristics of each reaction system are listed in Table S2.

tungsten-bis-(molybdopterin guanine dinucleotide) (W-bis-MGD), iron-sulfur (Fe-S) cluster, and flavin mononucleotide (FMN) as cofactors [41]. The reduction of CO_2 to formate by MeFDH1 was investigated using ethyl viologen (EV) as an electron mediator and carbon felt as the cathode in an H-type cell (Fig. 1). Cyclic voltammetry (CV) analysis revealed that, in the absence of both MeFDH1 and CO_2 purging (Fig. 2a), the electron mediator (EV) displayed a pair of reversible peaks corresponding to a one-electron redox transition at approximately −0.106 V versus the reversible hydrogen electrode (RHE). The half-wave potential of EV was marginally more negative than the standard reduction potential for CO_2 to formate (-0.053 V) [42]. The reversible CV profile of EV even in the presence of dissolved CO_2, indicates its exclusive function as an electron mediator without reactivity for CO_2 within a potential range. Additionally, the significantly reduced profile of MeFDH1 with CO_2 and EV demonstrates that MeFDH1 catalyzes CO_2 reduction using supplied electrons from reduced $EV^{\bullet+}$, in accordance with the reaction system designed in Fig. 1 (Fig. 2a, red line). The initial formate productivity escalated from 2.43 (± 0.15) mM/h at −0.014 V to 20.17 (± 2.03) mM/h at −0.214 V, representing a considerably high productivity via bioelectrocatalysis (Table S2) [43–45]. Further increases were not observed at more negative potentials, possibly due to limited solubility and mass transport of CO_2 in the electrolyte solution (Fig. 2b).

The exceptional formate yield achieved through the utilization of MeFDH1 highlights its superior efficiency in catalyzing the reduction of CO_2 to formate compared to the majority of other reported FDHs [46, 47]. Notably, the Faradaic efficiency of the formate synthesis process maintained at approximately 100% across all applied biases, ranging from −0.014 to −0.364 V. This contrasts significantly with traditional inorganic catalysts, often engage in undesired side reactions, leading to the production of hydrogen (H_2) and/or carbon monoxide (CO) [48,49]. The unique tunnels structures for CO_2 and formate, along with the intriguing metal coordination of the active site (W-*bis*-MGD) [50] may explain its superior performance in terms of activity levels, operational voltages, and Faradaic efficiency.

The kinetic efficiency for CO_2 reduction (k_{eff}) [37] was calculated by considering both turnover rates and substrate affinities to CO_2 and electron mediators. ICP-OES results for enzyme metal content refined this kinetic analysis of MeFDH1 and RcFDH, providing a precise determination of turnover activity at the active site involving W- or Mo-*bis*-MGD (Table S3). The k_{eff} value of MeFDH1 was approximately 4.02×10^6, which is remarkably higher than that of most reported FDHs, ranging from 1.8- to 10^{11}-folds between RcFDH and CbFDH (Table 1) [36,38]. The high turnover rate and the strong affinity with reduced $EV^{\bullet+}$ contributed to this exceptionally favorable k_{eff} for CO_2 reduction. The turnover rates of MeFDH1 for CO_2 reduction (k_{cat}) were 370.2 (±10.9) s^{-1} and 740.5 (± 21.8) s^{-1} for dissolved CO_2 and reduced $EV^{\bullet+}$, respectively (Fig. S2 and Table 1). The Michaelis-Menten constants (K_M) for dissolved CO_2 and reduced mediator ($EV^{\bullet+}$) were 3.903 (± 0.475) and 0.017 (± 0.002) mM, respectively, indicating that MeFDH1 efficiently catalyzes CO_2 reduction into formate with a strong affinity to the reducing mediator, despite its comparatively lower affinity to dissolved CO_2.

3.2. *Continuous CO_2 conversion of immobilized MeFDH1*

To enhance the long-term stability of biocatalytic CO_2 reduction, MeFDH1 was immobilized on agarose beads modified with nickel-nitrilotriacetic acid (Ni-NTA) by using a C-terminal His-tag on MeFDH1α (Fig. 3a). With free MeFDH1, formate rapidly reached 0.64 M at −0.164 V within 96 h; however, no further increase was observed thereafter (Fig. 3b). This was supposedly attributed to the denaturation of free MeFDH1 by shear stress caused by CO_2 bubbling [51]. In contrast, the immobilized enzyme enabled a steady increase in formate concentration up to 1.74 M for at 216 hours. Moreover, the immobilization did not exhibit any significant impact on the catalytic properties of the enzyme (Fig. S3). These results suggest that immobilization

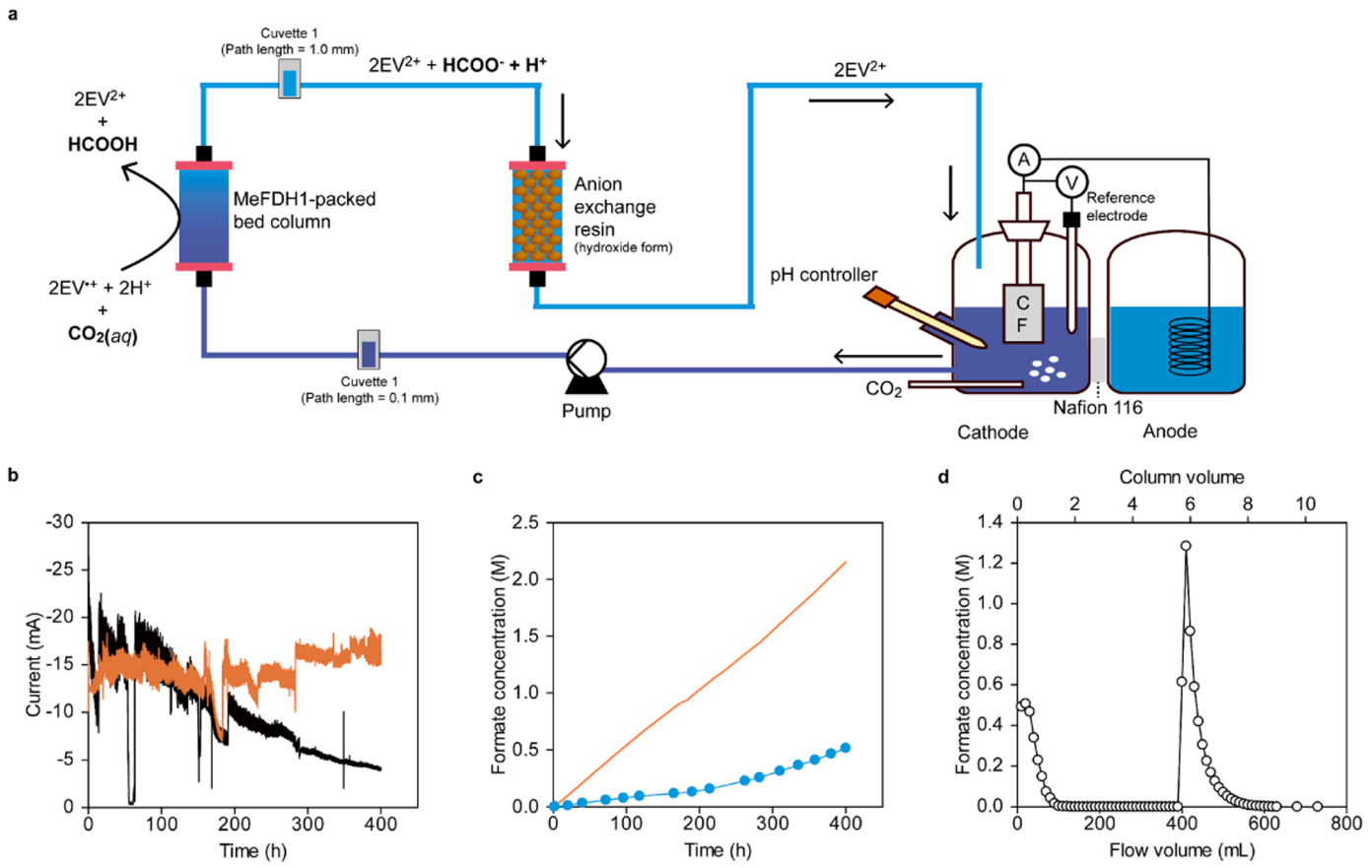

Fig. 4. Flow cell system of enzymatic CO_2 conversion with Anion-exchange resin (AIEX) column as in-situ separation unit. (a) Schematic representation of flow cell system with in-situ separation unit. (b) Current profile for formate production in the presence (orange line) and the absence (black line) of AIEX column. (c) The formate concentration in flowing electrolytes during long-term operation: Formate concentration measured in flowing electrolyte of cathode section (●) and estimated by current data (orange line). (d) Elute fractionation for formate desorption from AIEX column.

Table 1
Kinetic parameters of FDHs for CO_2 reduction.

FDHs	Substrates	k_{cat} (s^{-1})	K_M (mM)	k_{cat}/K_M($s^{-1}mM^{-1}$)	k_{eff}[a]
MeFDH1	Dissolved CO_2	370.2 (± 10.9)	3.903 (± 0.475)	94.87 (± 11.89)	4.02×10^6
	Reduced $EV^{\bullet+}$	740.5 (± 21.8)	0.017 (± 0.002)	42393 (± 4931)	
RcFDH[b]	Dissolved CO_2	67.00 (± 5.49)	0.250 (± 0.028)	268.0 (± 37.2)	2.24×10^6
	Reduced $EV^{\bullet+}$	134.0 (± 11.0)	0.016 (± 0.002)	8375 (± 1252)	
CnFDH[c] [36] (ReFDH)	Dissolved CO_2	11 (± 0.4)	2.7 (± 0.3)	4.07 (± 0.60)	9.73×10^2
	NADH	11 (± 0.4)	0.046 (± 0.004)	239 (± 29)	
TsFDH[d] [38]	Bicarbonate	0.318 (±0.051)	9.23 (±3.98)	0.034 (± 0.020)	4.08×10^{-2}
	NADH	0.318 (±0.051)	0.264 (±0.076)	1.2 (± 0.5)	
CbFDH[e] [38]	Bicarbonate	0.015 (±0.005)	31.28 (±8.05)	4.795×10^{-4} (± 2.04×10^{-4})	1.39×10^{-5}
	NADH	0.015 (±0.005)	0.512 (±0.186)	0.029 (± 0.020)	

a Kinetic efficiency for CO2 reduction, $k_{eff} = (k_{cat.CO_2} \text{ or } bicarbonate / K_{M.CO_2} \text{ or } bicarbonate)(k_{cat.EV^{\bullet+}} \text{ or } NADH / K_{M.EV^{\bullet+}} \text{ or } NADH)$
b-e Formate dehydrogenases (FDHs) from Rhodobacter capsulatus, Ralstonia eutropha (Cupriavidus necator) HF210, Thiobacillus sp, and Candida boidinii, respectively.

considerably enhances the stability of MeFDH1 for long-term applications [52]. Upon immobilization, MeFDH1 was readily recycled three times for repeated CO_2 reduction without any significant performance degradation in productivity or selectivity (Fig. 3c). Despite remarkable selectivity of enzymes, their insufficient stability and total turnover number have been noted as critical drawbacks [52,53]. Accordingly, the operating time and formate concentration of other FDH-catalyzed reaction systems utilizing electrochemical reactor or cascade reactions were compared with those of the present work. The reaction performance and stability of immobilized MeFDH1 expanded the applicability of enzymatic CO_2 conversion to formate on both activity and stability (Fig. 3d and Table S2). This comparison provides evidence for the breakthrough approach of enzymatic CO_2 conversion, demonstrating suitable reducing power and enzyme characteristics are critical molar-scale formate production over long-term period.

3.3. Flow reactor system of MeFDH1-catalzyzed CO_2 reduction with in-situ separation unit

Building upon the enhanced stability achieved through immobilization, we designed a flow reactor system integrating a plug flow reactor (PFR) with immobilized MeFDH1 to expand the potential for long-term stability and operational flexibility. This system not only lessened dependence on electrolysis performance but also provided the benefit of independent modulation and efficient integration of extra operational units, such as separation processes, facilitating a significant improvement in overall system performance. Without a separation unit, the flow reactor system achieved a formate concentration of 1.7 M, which plateaued after 500 hours, maintaining a nearly perfect Faradaic efficiency of 100.3% (Fig. S4). To investigate the saturation profile, formate concentrations ranging from 0 to 0.99 M were deliberately introduced during the electrochemical batch reaction system. Intriguingly, the current declined from −42 to −15 mA proportionally across this range (Fig. S5), which implies that MeFDH1 is subject to product inhibition during CO_2 reduction reaction, resulting in the gradual decrease of CO_2 reduction rate. These findings suggested in-situ separation of product from flowing electrolytes to repress product inhibition during enzymatic CO_2 conversion.

MeFDH1-packed plug flow reactor with an in-situ separation unit was prepared by positioning an anion exchange (AIEX) column between the MeFDH1-packed PFR and the cathode cell to separate the formate generated by MeFDH1 immediately (Fig. 4a and S6). Anion exchange resin (AIEX, Ambersep 900®) was chosen for the separation unit, as it enables selective adsorption of the negatively charged product from the positively charged electron mediator ($EV^{\bullet+}/EV^{2+}$). While the current of the flow reactor without an AIEX column declined steadily from −20 to −5 mA, the flow reactor equipped with an AIEX column demonstrated the ability to maintain its initial current (Fig. 4b). Real-time monitoring of reduced $EV^{\bullet+}$ concentration in the flowing electrolytes revealed an immediate increase of up to 21 hours at both the inlet and outlet of MeFDH1-packed PFR, followed by stabilization in accordance with the current profile. (Fig. 4b and S7). To assess the adsorption efficiency of the AIEX column during actual formate production, the concentration of formate in the electrolytes was determined using high performance liquid chromatography (HPLC). It was observed that approximately 24% of the expected formate concentration based on the current remained in the electrolytes, despite the utilization of a sufficient quantity of AIEX beads loaded to adsorb formate within the anticipated range of production (Fig. 4c). Considering bicarbonate generated from CO_2 purging as a potential candidate for competitive adsorption, it may interfere with the selective adsorption of formate due to its negative charge. Hence, further study will be necessary to optimize the selective adsorption of formate. After a long-term operation of enzymatic CO_2 conversion of 400 hours, the AIEX column was detached from the flow reactor system to verify the recovery efficiency of the produced formate. With the eluent of 1 N-NaOH through the AIEX column, a distinct and sharp peak of elution was observed in the eluate fractionation (Fig. 4e). Eventually, a total of 107.7 mmol of formate was obtained from the long-term operation of enzymatic CO_2 conversion, with a recovery efficiency of 99.5% (Table S4). This study on flow reactor system clearly suggests that produced formate is separated by the adsorption on AIEX resin from flowing electrolyte and highly concentrated formate could be efficienclty recovered by the elution step of an AIEX column after the end of long-term operation of CO_2 conversion.

4. Conclusion

To summarize, we demonstrate that employing MeFDH1 can overcome three major challenges in CO_2 reduction to formate using biocatalysts: low activity, low productivity, and low long-term operational stability. As a result, more than 1.7 M of formate was produced at an initial rate of approximately 20 mM/h with near-unity Faradaic efficiency for over 200 h. Furthermore, its flow reactor system presented scalability and applicability of enzymatic CO_2 conversion, including a noteworthy strategy for product separation with sufficient efficiency. This discovery lays the foundation for an efficient CO_2 reduction process that could potentially address the pressing issue of global warming in the future.

CRediT authorship contribution statement

Yong Hwan Kim: Writing – review & editing, Project administration, Investigation, Funding acquisition, Conceptualization. **Jungki Ryu:** Writing – original draft, Formal analysis, Data curation. **Uyen Thu Phan:** Writing – original draft, Investigation, Data curation. **Byoung Wook Jeon:** Writing – original draft, Methodology, Investigation, Data curation. **Hyung Ho Lee:** Writing – review & editing. **Yoonyoung Heo:** Methodology, Investigation.

Declaration of Competing Interest

The authors declare that they have no known competing financial interests or personal relationships that could have appeared to influence the work reported in this paper.

Data Availability

No data was used for the research described in the article.

Acknowledgements

This work was supported by Korea NRF CGRC (2015M3D3A1A01064919), ERC (2020R1A5A1019631), KEIT (1415184376) and US DOE NETL (DE-FE0031720), We thank UCRF (UNIST Central Research Facilities) for support of using the equipment.

Appendix A. Supporting information

Supplementary data associated with this article can be found in the online version at doi:10.1016/j.jcou.2024.102754.

References

[1] Y.Y. Birdja, E. Pérez-Gallent, M.C. Figueiredo, A.J. Göttle, F. Calle-Vallejo, M. T. Koper, Advances and challenges in understanding the electrocatalytic conversion of carbon dioxide to fuels, Nat. Energy 4 (9) (2019) 732–745.
[2] W. Lai, Y. Qiao, J. Zhang, Z. Lin, H. Huang, Design strategies for markedly enhancing energy efficiency in the electrocatalytic CO_2 reduction reaction, Energy Environ. Sci. 15 (9) (2022) 3603–3629.
[3] K. Sordakis, C. Tang, L.K. Vogt, H. Junge, P.J. Dyson, M. Beller, G. Laurenczy, Homogeneous catalysis for sustainable hydrogen storage in formic acid and alcohols, Chem. Rev. 118 (2) (2018) 372–433.
[4] J. Bang, C.H. Hwang, J.H. Ahn, J.A. Lee, S.Y. Lee, *Escherichia coli* is engineered to grow on CO_2 and formic acid, Nat. Microbiol. 5 (12) (2020) 1459–1463.
[5] O. Yishai, S.N. Lindner, J.G. de la Cruz, H. Tenenboim, A. Bar-Even, The formate bio-economy, Curr. Opin. Chem. Biol. 35 (2016) 1–9.
[6] H.W. Hwang, J. Yoon, K. Min, M.-S. Kim, S.-J. Kim, D.H. Cho, H. Susila, J.-G. Na, M.-K. Oh, Y.H. Kim, Two-stage bioconversion of carbon monoxide to biopolymers via formate as an intermediate, Chem. Eng. J. 389 (2020) 124394.
[7] F. Humpenöder, B.L. Bodirsky, I. Weindl, H. Lotze-Campen, T. Linder, A. Popp, Projected environmental benefits of replacing beef with microbial protein, Nature 605 (7908) (2022) 90–96.
[8] M. Sakarika, P. Candry, M. Depoortere, R. Ganigué, K. Rabaey, Impact of substrate and growth conditions on microbial protein production and composition, Bioresour. Technol. 317 (2020) 124021.
[9] A.M. Ochsner, F. Sonntag, M. Buchhaupt, J. Schrader, J.A. Vorholt, Methylobacterium extorquens: methylotrophy and biotechnological applications, Appl. Microbiol. Biotechnol. 99 (2015) 517–534.
[10] D. Wei, R. Sang, P. Sponholz, H. Junge, M. Beller, Reversible hydrogenation of carbon dioxide to formic acid using a Mn-pincer complex in the presence of lysine, Nat. Energy 7 (5) (2022) 438–447.
[11] S. Chatterjee, I. Dutta, Y. Lum, Z. Lai, K.-W. Huang, Enabling storage and utilization of low-carbon electricity: power to formic acid, Energy Environ. Sci. 14 (3) (2021) 1194–1246.

[12] X. Min, M.W. Kanan, Pd-catalyzed electrohydrogenation of carbon dioxide to formate: high mass activity at low overpotential and identification of the deactivation pathway, J. Am. Chem. Soc. 137 (14) (2015) 4701–4708.

[13] Y. Hori, H. Wakebe, T. Tsukamoto, O. Koga, Electrocatalytic process of CO selectivity in electrochemical reduction of CO_2 at metal electrodes in aqueous media, Electrochim. Acta 39 (11-12) (1994) 1833–1839.

[14] L. Fan, C. Xia, P. Zhu, Y. Lu, H. Wang, Electrochemical CO_2 reduction to high-concentration pure formic acid solutions in an all-solid-state reactor, Nat. Commun. 11 (1) (2020) 3633.

[15] C. Xia, P. Zhu, Q. Jiang, Y. Pan, W. Liang, E. Stavitski, H.N. Alshareef, H. Wang, Continuous production of pure liquid fuel solutions via electrocatalytic CO_2 reduction using solid-electrolyte devices, Nat. Energy 4 (9) (2019) 776–785.

[16] S. Van Daele, L. Hintjens, S. Hoekx, B. Bohlen, S. Neukermans, N. Daems, J. Hereijgers, T. Breugelmans, How flue gas impurities affect the electrochemical reduction of CO2 to CO and formate, Appl. Catal. B-Environ. 341 (2024) 123345.

[17] W. Luc, B.H. Ko, S. Kattel, S. Li, D. Su, J.G. Chen, F. Jiao, SO_2-induced selectivity change in CO_2 electroreduction, J. Am. Chem. Soc. 141 (25) (2019) 9902–9909.

[18] B.H. Ko, B. Hasa, H. Shin, E. Jeng, S. Overa, W. Chen, F. Jiao, The impact of nitrogen oxides on electrochemical carbon dioxide reduction, Nat. Commun. 11 (1) (2020) 5856.

[19] K. Fernández-Caso, G. Díaz-Sainz, M. Alvarez-Guerra, A. Irabien, Electroreduction of CO_2: advances in the continuous production of formic acid and formate, ACS Energy Lett. 8 (4) (2023) 1992–2024.

[20] Y. Kuang, H. Rabiee, L. Ge, T.E. Rufford, Z. Yuan, J. Bell, H. Wang, High-concentration electrosynthesis of formic acid/formate from CO_2: reactor and electrode design strategies, Energy Environ. Mater. 6 (6) (2023) e12596.

[21] T. Fan, W. Ma, M. Xie, H. Liu, J. Zhang, S. Yang, P. Huang, Y. Dong, Z. Chen, X. Yi, Achieving high current density for electrocatalytic reduction of CO_2 to formate on bismuth-based catalysts, Cell Rep. Phys. Sci. 2 (3) (2021).

[22] I. Grigioni, L.K. Sagar, Y.C. Li, G. Lee, Y. Yan, K. Bertens, R.K. Miao, X. Wang, J. Abed, D.H. Won, F.P. García de Arquer, A.H. Ip, D. Sinton, E.H. Sargent, CO_2 electroreduction to formate at a partial current density of 930 mA cm–2 with InP colloidal quantum dot derived catalysts, ACS Energy Lett. 6 (1) (2020) 79–84.

[23] L. Fan, C. Xia, P. Zhu, Y. Lu, H. Wang, Electrochemical CO_2 reduction to high-concentration pure formic acid solutions in an all-solid-state reactor, Nat. Commun. 11 (1) (2020) 3633.

[24] A. Bassegoda, C. Madden, D.W. Wakerley, E. Reisner, J. Hirst, Reversible interconversion of CO_2 and formate by a molybdenum-containing formate dehydrogenase, J. Am. Chem. Soc. 136 (44) (2014) 15473–15476.

[25] H. Chen, O. Simoska, K. Lim, M. Grattieri, M. Yuan, F. Dong, Y.S. Lee, K. Beaver, S. Weliwatte, E.M. Gaffney, Fundamentals, applications, and future directions of bioelectrocatalysis, Chem. Rev. 120 (23) (2020) 12903–12993.

[26] B.A. Parkinson, P.F. Weaver, Photoelectrochemical pumping of enzymatic CO_2 reduction, Nature 309 (5964) (1984) 148–149.

[27] K.P. Sokol, W.E. Robinson, A.R. Oliveira, J. Warnan, M.M. Nowaczyk, A. Ruff, I.A. C. Pereira, E. Reisner, Photoreduction of CO_2 with a formate dehydrogenase driven by photosystem II using a semi-artificial Z-scheme architecture, J. Am. Chem. Soc. 140 (48) (2018) 16418–16422.

[28] L.B. Maia, L. Fonseca, I. Moura, J.J.G. Moura, Reduction of carbon dioxide by a molybdenum-containing formate dehydrogenase: a kinetic and mechanistic study, J. Am. Chem. Soc. 138 (28) (2016) 8834–8846.

[29] E.-G. Choi, Y.J. Yeon, K. Min, Y.H. Kim, Communication—CO_2 reduction to formate: an electro-enzymatic approach using a formate dehydrogenase from *Rhodobacter capsulatus*, J. Electrochem. Soc. 165 (9) (2018) H446–H448.

[30] H. Hwang, Y.J. Yeon, S. Lee, H. Choe, M.G. Jang, D.H. Cho, S. Park, Y.H. Kim, Electro-biocatalytic production of formate from carbon dioxide using an oxygen-stable whole cell biocatalyst, Bioresour. Technol. 185 (2015) 35–39.

[31] J. Jang, B.W. Jeon, Y.H. Kim, Bioelectrochemical conversion of CO_2 to value added product formate using engineered *Methylobacterium extorquens*, Sci. Rep. 8 (1) (2018) 7211.

[32] U.T. Phan, B.W. Jeon, Y.H. Kim, Microbial engineering of Methylorubrum extorquens AM1 to enhance CO2 conversion into formate, Enzym. Microb. Technol. 168 (2023) 110264.

[33] C.J. Marx, M.E. Lidstrom, Broad-host-range *cre-lox* system for antibiotic marker recycling in gram-negative bacteria, Biotechniques 33 (5) (2002) 1062–1067.

[34] C.J. Marx, M.E. Lidstrom, Development of improved versatile broad-host-range vectors for use in methylotrophs and other Gram-negative bacteria, Microbiology 147 (8) (2001) 2065–2075.

[35] R. Peyraud, P. Kiefer, P. Christen, S. Massou, J.-C. Portais, J.A. Vorholt, Demonstration of the ethylmalonyl-CoA pathway by using ^{13}C metabolomics, Proc. Natl. Acad. Sci. U. S. A 106 (12) (2009) 4846–4851.

[36] X. Yu, D. Niks, A. Mulchandani, R. Hille, Efficient reduction of CO_2 by the molybdenum-containing formate dehydrogenase from *Cupriavidus necator* (*Ralstonia eutropha*), J. Biol. Chem. 292 (41) (2017) 16872–16879.

[37] R.H. Ringborg, J. Woodley, The application of reaction engineering to biocatalysis, Reac. Chem. Eng. 1 (1) (2016) 10–22.

[38] H. Choe, J.C. Joo, D.H. Cho, M.H. Kim, S.H. Lee, K.D. Jung, Y.H. Kim, Efficient CO_2-reducing activity of NAD-dependent formate dehydrogenase from *Thiobacillus* sp. KNK65MA for formate production from CO_2 gas, PLoS One 9 (7) (2014) e103111.

[39] M. Laukel, L. Chistoserdova, M.E. Lidstrom, J.A. Vorholt, The tungsten-containing formate dehydrogenase from *Methylobacterium extorquens* AM1: purification and properties, Eur. J. Biochem. 270 (2) (2003) 325–333.

[40] M. Miller, W.E. Robinson, A.R. Oliveira, N. Heidary, N. Kornienko, J. Warnan, I.A. C. Pereira, E. Reisner, Interfacing formate dehydrogenase with metal oxides for the reversible electrocatalysis and solar-driven reduction of carbon dioxide, Angew. Chem., Int. Ed. 58 (14) (2019) 4601–4605.

[41] T. Yoshikawa, F. Makino, T. Miyata, Y. Suzuki, H. Tanaka, K. Namba, K. Kano, K. Sowa, Y. Kitazumi, O. Shirai, Multiple electron transfer pathways of tungsten-containing formate dehydrogenase in direct electron transfer-type bioelectrocatalysis, Chem. Commun. 58 (45) (2022) 6478–6481.

[42] R.K. Thauer, K. Jungermann, K. Decker, Energy conservation in chemotrophic anaerobic bacteria, Bacteriol. Rev. 41 (1) (1977) 100–180.

[43] S.J. Cobb, V.M. Badiani, A.M. Dharani, A. Wagner, S. Zacarias, A.R. Oliveira, I.A. C. Pereira, E. Reisner, Fast CO_2 hydration kinetics impair heterogeneous but improve enzymatic CO_2 reduction catalysis, Nat. Chem. 14 (4) (2022) 417–424.

[44] R. Wu, F. Li, X. Cui, Z. Li, C. Ma, H. Jiang, L. Zhang, Y.-H.P.J. Zhang, T. Zhao, Y. Zhang, Y. Li, H. Chen, Z. Zhu, Enzymatic electrosynthesis of glycine from CO_2 and NH_3, Angew. Chem., Int. Ed. 62 (14) (2023) e202218387.

[45] M. Baccour, A. Lamotte, K. Sakai, E. Dubreucq, A. Mehdi, K. Kano, A. Galarneau, J. Drone, N. Brun, Production of formate from CO_2 gas under ambient conditions: towards flow-through enzyme reactors, Green. Chem. 22 (12) (2020) 3727–3733.

[46] S.Y. Lee, S.Y. Lim, D. Seo, J.Y. Lee, T.D. Chung, Light-driven highly selective conversion of CO_2 to formate by electrosynthesized enzyme/cofactor thin film electrode, Adv. Energy Mater. 6 (11) (2016) 1502207.

[47] S.K. Kuk, Y. Ham, K. Gopinath, P. Boonmongkolras, Y. Lee, Y.W. Lee, S. Kondaveeti, C. Ahn, B. Shin, J.-K. Lee, S. Jeon, C.B. Park, Continuous 3D titanium nitride nanoshell structure for solar-driven unbiased biocatalytic CO_2 reduction, Adv. Energy Mater. 9 (25) (2019) 1900029.

[48] T. Kawawaki, T. Okada, D. Hirayama, Y. Negishi, Atomically precise metal nanoclusters as catalysts for electrocatalytic CO_2 reduction, Green. Chem. 26 (2024) 122–163.

[49] Y.-J. Ko, J.-Y. Kim, W.H. Lee, M.G. Kim, T.-Y. Seong, J. Park, Y. Jeong, B.K. Min, W.-S. Lee, D.K. Lee, H.-S. Oh, Exploring dopant effects in stannic oxide nanoparticles for CO_2 electro-reduction to formate, Nat. Commun. 13 (1) (2022) 2205.

[50] J.Y. Yang, T.A. Kerr, X.S. Wang, J.M. Barlow, Reducing CO_2 to HCO_2^- at mild potentials: lessons from formate dehydrogenase, J. Am. Chem. Soc. 142 (46) (2020) 19438–19445.

[51] S.R. Anderson, B.R. Bommarius, J.M. Woodley, A.S. Bommarius, Sparged but not stirred: rapid, ADH-NADH oxidase catalyzed deracemization of alcohols in a bubble column, Chem. Eng. J. 417 (2021) 127909.

[52] A.S. Bommarius, M.F. Paye, Stabilizing biocatalysts, Chem. Soc. Rev. 42 (15) (2013) 6534–6565.

[53] M. Moon, G.W. Park, J.-p Lee, J.-S. Lee, K. Min, Recent progress in formate dehydrogenase (FDH) as a non-photosynthetic CO_2 utilizing enzyme: a short review, J. CO2 Util. 42 (2020) 101353.